Article

Enhancement of Methane Detection in Tunable Diode Laser Absorption Spectroscopy Using Savitzky–Golay Filtering

Shichao Chen [1,2,*]**, Xing Tian** [1,2,3,*]**, Tong Mu** [1,2]**, Jun Yuan** [1,2]**, Xile Cao** [1,2] **and Gang Cheng** [3]

1 The First Affiliated Hospital of Anhui University of Science and Technology (Huainan First People's Hospital), Anhui University of Science and Technology, Huainan 232001, China; 15178219810@163.com (T.M.); yuanjun1186196986@163.com (J.Y.); caoxile2024624@163.com (X.C.)
2 School of Artificial Intelligence, Anhui University of Science and Technology, Huainan 232001, China
3 State Key Laboratory of Mining Response and Disaster Prevention and Control in Deep Coal Mines, Anhui University of Science and Technology, Huainan 232001, China; chgmech@mail.ustc.edu.cn
* Correspondence: csc18856683605@163.com (S.C.); 2019018@aust.edu.cn (X.T.)

Abstract: In order to enhance gas absorption efficiency and improve the detection sensitivity of methane, a gas absorption cell with an effective optical path length of 29.37 m was developed, employing tunable diode laser absorption spectroscopy (TDLAS) and a distributed feedback (DFB) laser with a center wavelength of 1.654 μm as the light source. However, despite these advancements, the detection accuracy was still limited by potential signal interference and noise. To address these challenges, the Savitzky–Golay (S-G) filtering technique was implemented to optimize the TDLAS detection signal. Experimental results indicated a significant enhancement in detection performance. For a methane concentration of 92 ppm, the application of the S-G filter improved the signal-to-noise ratio by a factor of 1.84, resulting in a final device detection accuracy of 0.53 ppm. This improvement demonstrates the effectiveness of the S-G filter in enhancing detection sensitivity, supporting high-precision methane monitoring for atmospheric analysis and various industrial applications.

Keywords: TDLAS; Savitzky–Golay; signal-to-noise ratio; detection limit

1. Introduction

With the growing emphasis on environmental protection and renewable energy worldwide, methane, as a potent greenhouse gas, has garnered significant attention due to its role in global warming and climate change. Methane emissions, primarily originating from energy conversion processes, industrial production, and agricultural activities, have a substantial impact on climate dynamics, thereby driving an increasing need for effective and real-time monitoring of methane concentrations [1–3].Traditional methane detection methods, such as gas chromatography and catalytic combustion, often face challenges due to constraints imposed by environmental factors, including variations in temperature and humidity, as well as limitations in equipment sensitivity and response time. These limitations can significantly hinder the ability to achieve high-precision and high-sensitivity methane detection, especially in dynamic or harsh environmental conditions. Moreover, traditional methods typically require complex sample pretreatment, which limits their applicability for real-time and in situ monitoring purposes [4].

In light of these challenges, the development and refinement of novel methane detection technologies have become crucial. Tunable diode laser absorption spectroscopy (TDLAS), characterized by its high sensitivity, selectivity, and fast response, has emerged

as a leading technique for methane detection in complex environments. These characteristics render TDLAS a powerful tool for gas analysis, exploiting the unique infrared absorption spectra of target molecules for precise and reliable measurements. Over the past few years, substantial research has showcased the effectiveness of TDLAS for methane detection, underscoring its potential in achieving high-precision environmental monitoring and advancing related fields [5–7]. In the TDLAS, the optical multi-pass absorption cell is one of the key equipment. The design principle of the multi-pass absorption cell is based on limiting the incident light to reflect back and forth between two or more highly reflective mirrors, thereby increasing the effective optical path of the light–substance interaction to obtain the absorption spectral signal with a high signal-to-noise ratio (SNR), thus realizing high sensitivity measurement of trace gases at low concentrations. In a certain volume and physical size of the optical multi-pass absorption cell, the number of reflections is increased as much as possible to improve the effective optical path, but because they are easily affected by light overlap resulting in light path interference, the reflections will ultimately affect the detection sensitivity and accuracy of the measurement system. Additionally, noise generated by sensors, detectors, and other electronic devices can increase the uncertainty in the signal processing process. Even with high-precision instruments, the detection of low-concentration methane may still be limited by noise. These limitations seriously hinder the ability to achieve high precision and sensitivity in methane detection, especially under dynamic or harsh environmental conditions [8–11].

Addressing these challenges requires effective signal processing and optimization strategies, which have become the focus of research in gas sensing technology. One such promising technique is the Savitzky–Golay filter, which is a powerful signal smoothing algorithm widely used in data analysis [12,13]. Compared with conventional filters such as moving average filters and low-pass filters, Savitzky–Golay filters can well retain the basic features of the original signal, such as peak shape and peak width, and also effectively reduce the noise and improve the signal-to-noise ratio (SNR). It is therefore particularly suitable for quantitative spectroscopic analysis where maintaining signal integrity is essential for accurate concentration calculations. The Savitzky–Golay filter technique has been successful in a number of fields including analytical chemistry, biomedical signal analysis, and environmental monitoring, providing a valuable method for the detection of methane using TDLAS. The integration of this filtering technique into the methane TDLAS detection framework has been shown to be effective in improving the measurement accuracy and reliability [14–16]. For instance, Ji et al. [17] combined wavelet denoising (WD) and Savitzky–Golay (SG) to improve the performance of a methane sensor to process the noisy signal, and the SNR of the absorbance signal was improved by a factor of 4.95 with the wavelet denoising and Savitzky–Golay filtering scheme. The 1 sigma limit of detection of the sensor is reduced from 2929 ppm to 397 ppm, according to the Allan deviation analysis. By mitigating environmental and instrumental noise, the method improves the SNR, allowing for a lower detection limit and increased sensitivity. Such advancements are vital for real-time environmental monitoring and industrial safety, where high precision and reliability are essential. Thus, incorporating advanced signal processing techniques, such as the Savitzky–Golay filter, is a significant step towards optimizing TDLAS-based methane detection, ultimately leading to more accurate and effective monitoring of methane emissions.

This study presents the development of a methane detection system based on tunable diode laser absorption spectroscopy, incorporating a novel, compact, dense-pattern multi-pass gas cell with an effective optical path length of 29.37 m. A near-infrared distributed feedback (DFB) diode laser operating at a wavelength of 1.654 μm was utilized as the light source. To further enhance the detection performance, the Savitzky–Golay (S-G) filtering technique was employed, leading to an improvement in the signal-to-noise ratio (SNR)

by a factor of 1.84. Consequently, the system has a detection accuracy of 0.53 ppm when measuring a methane concentration of 92 ppm, indicating its potential for high-precision methane monitoring in both environmental and industrial applications.

2. Experimental Details

A schematic diagram of the experimental setup is shown in Figure 1. The light source for the system is a distributed feedback (DFB) diode laser operating at a wavelength of 1.654 μm and at room temperature. To ensure stable and precise operation, the laser current and temperature were controlled using a commercial diode laser controller (Model LDC 501, Stanford Research Systems, Sunnyvale, CA, USA), which maintained a constant operating temperature of 22 °C and a driving current of 85 mA. To achieve wavelength scanning, an external voltage ramp from a function generator (DG4162, RIGOL, Beijing, China) was applied to the laser diode current. This ramp modulated the laser wavelength back and forth across the absorption line with a peak amplitude of 1 V and a scanning frequency of 100 Hz, allowing precise control of the laser emission over the desired spectral range. The laser beam was collimated with a fiber-coupled collimator and subsequently injected into the compact dense-pattern multi-pass gas cell. Inside the multi-pass cell, the laser beam was reflected 243 times between two concave mirrors, resulting in an effective optical path length of 29.37 m, which significantly enhances the sensitivity of the system by increasing the interaction time between the laser and the target gas [18]. After passing through the gas cell, the output beam was focused onto a photodetector (PDA20CS-EC, Thorlabs, Newton, NJ, USA) using a lens with a focal length of 50 mm. The photodetector converted the optical signal into an electrical signal, which was then digitized by a data acquisition (DAQ) card (NI USB-6210, National Instruments, Austin, TX, USA). The acquired data were displayed and analyzed in real-time on a laptop using a LabVIEW NXG 5.0 interface, providing immediate feedback for monitoring and further analysis.
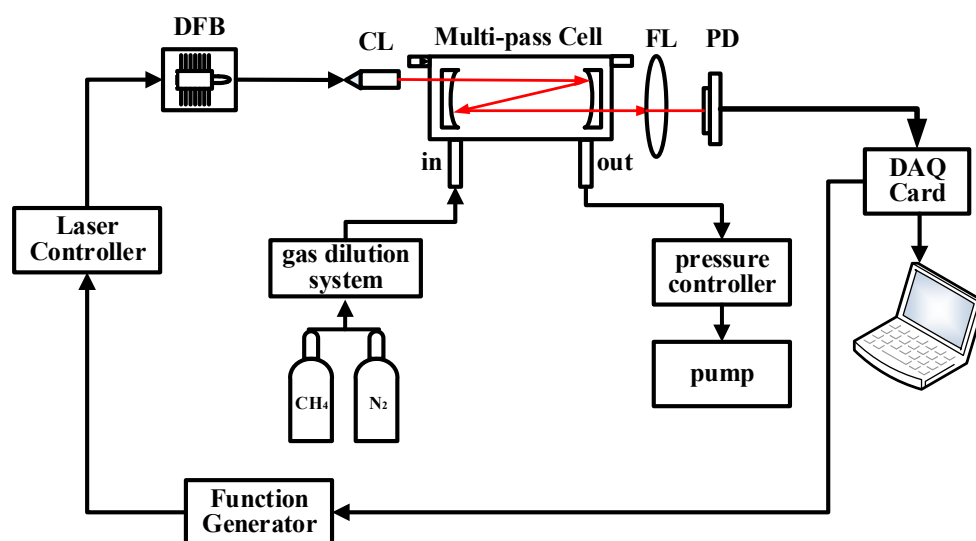

Figure 1. Schematic diagram of experimental device of measurement system. CL: collimator; FL: focusing lens; PD: photodetector.

3. Results and Discussion

3.1. Selection of CH_4 Absorption Lines

According to the HITRAN 2016 database, the best CH_4 absorption lines within the spectral tuning range of the used 1.654 μm diode laser are the R3 triplet of the $2v_3$ band near 6046.96 cm^{-1}. These lines exhibit the highest absorption intensities and are free from significant interference by other molecules, such as H_2O and CO_2. In the experimental

setup, the three individual spectral lines of the R3 triplet are approximated as a single spectral line for processing purposes. The line strength used for analysis is taken as the average of the absorption strengths of these three lines [19,20]. Figure 2 shows simulated absorption spectra of 492 ppm CH_4 near the 6046.96 cm^{-1} at a pressure of 0.5 atm. The laser center current was set at 85 mA with a temperature set at 22 °C for targeting the selected CH_4 absorption lines. The figure also illustrates the relationship between the applied current and the corresponding wavenumber, which is crucial for calibrating the system and ensuring accurate methane concentration measurements.
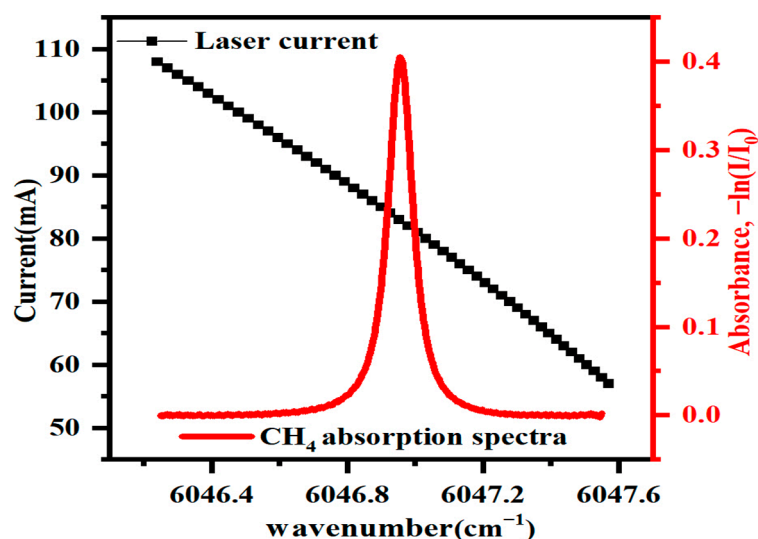
Figure 2. The simulated CH_4 absorption coefficient spectrum and the relationship between the laser injection current and the wavenumber.

3.2. The Measured Signal of CH_4

In the experiment, five groups of CH_4 gases with different concentrations of 92 ppm, 192 ppm, 292 ppm, 392 ppm, and 492 ppm were configured with the distribution system, and the CH_4 absorption spectrum was obtained at the pressure of 0.5 atm and the room temperature of 23.4 °C, as shown in Figure 3a. Figure 3b illustrates the linear fitting relationship between the integrated absorption area of CH_4 and its concentration. A strong linear correlation was observed, with a correlation coefficient of 99.98%, indicating a high degree of accuracy in the measurement. This result demonstrates that the system can be effectively calibrated by inverting the integrated absorption area to determine the corresponding gas concentration. The precise linearity of this relationship further suggests that the system is reliable for quantitative CH_4 detection across a wide concentration range.

3.3. Savitzky–Golay Smoothing

To verify the feasibility of Savitzky–Golay (S-G) filtering for spectral denoising, a simulation of a methane (CH_4) weak absorption line was conducted using MATLAB R2024b. First, the direct absorption spectrum (DAS) signal was superimposed with interference noise and white noise to generate a noisy signal. The noisy signal is shown in Figure 4a. To evaluate the denoising performance, signal-to-noise ratio (SNR), root mean square error (RMSE), and correlation coefficient (CC) were used as metrics to assess the correlation between the noisy signal and the denoised signal. These indicators were further analyzed to study the effectiveness of the filtering process.
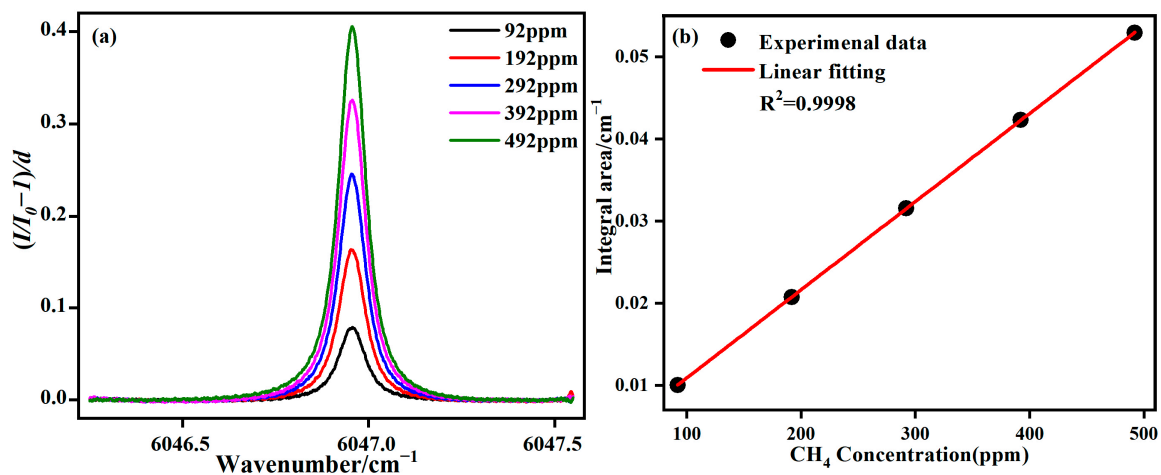
Figure 3. (**a**) The absorption coefficient spectra of methane at different concentrations. (**b**) The integral area curve of methane at different concentrations.
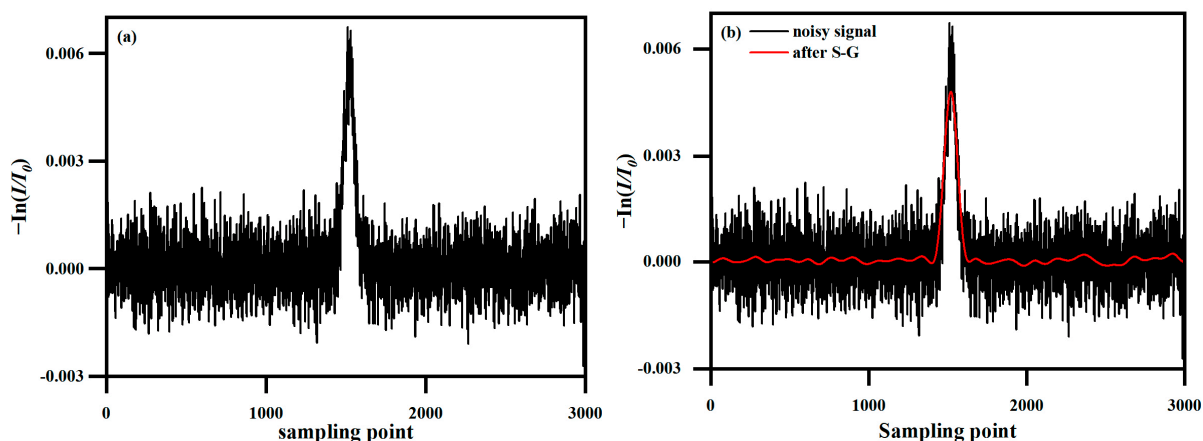

Figure 4. (**a**) Graph of the noisy signal. (**b**) Comparison with the original signal after S-G denoising.

For the noisy signal, S-G filtering was applied. Given that the SNR was close to 1, and the noise level was high, a larger window size was selected to enhance the denoising effect. Since methane detection signals are typically continuous and smooth, and a second-order polynomial (i.e., parabola) can effectively fit the smooth variations in local regions, a quadratic polynomial was chosen for fitting. The comparison between the filtered signal and the original signal is shown in Figure 4b. The calculated RMSE between the two signals was 0.0067%, SNR was 20.95, and CC was 99.5979%, demonstrating that the S-G filter effectively reduces noise.

Then, to further enhance the signal-to-noise ratio (SNR) of methane absorption signals and achieve a smoother absorption spectrum, the collected spectral data were post-processed using the Savitzky–Golay (S-G) convolution smoothing algorithm. The S-G algorithm operates by performing discrete processing, which involves weighted averaging within a sliding window. The weighting coefficients are determined by fitting a least squares polynomial within the window, enabling effective noise reduction while preserving the higher-order derivative characteristics of the data. In this study, to optimize the parameters of the Savitzky–Golay algorithm, a second-order polynomial was employed for fitting. Five different window widths (20, 40, 60, 40, 80, and 100) were evaluated on a methane signal with a concentration of 92 ppm, as illustrated in Figure 5. The results indicated that as the window width increased, the smoothing effect on the spectral line became more pronounced. However, an excessively large window width led to the loss

of key spectral features, which are critical for accurate detection and quantification. To balance the trade-off between effective noise reduction and the preservation of important spectral details, a window width of 60 was selected as optimal for processing the spectral data using the S-G algorithm. The results show that the smoothing effect on the spectral lines becomes more and more obvious as the window width increases. However, an excessively large window width led to the loss of key spectral features, which are critical for accurate detection and quantification. In order to strike a balance between effective noise reduction and retention of important spectral detailing, an optimal window width of 60 was selected as optimal for processing the spectral data using the S-G algorithm to avoid signal distortion as the signal peaks flatten out at window widths of 80 and 100, and a noticeable distortion occurs.
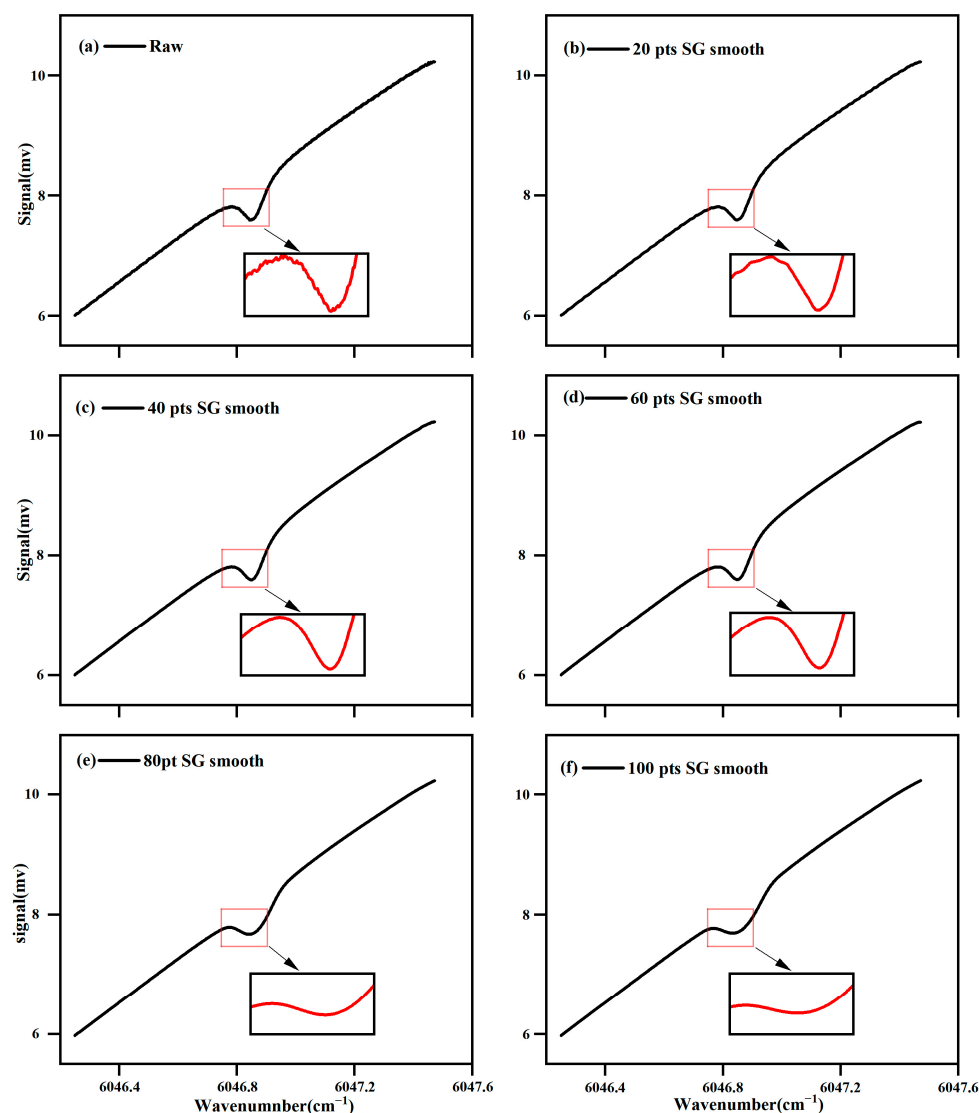
Figure 5. (**a**) Original absorption spectrum data. (**b**–**f**) The results of Savitzky–Golay smoothing with different window widths ranging from 20 to 100.

3.4. Performance Evaluation

To evaluate the performance of the CH_4 sensor, we analyze both the integrated area of CH_4 and the standard deviation of the fitting residuals at a concentration of 92 ppm, as illustrated in Figure 6. In Figure 6a, the original data yields a signal-to-noise ratio (SNR) of 93.41, and the detection accuracy of the device is 0.98 ppm, indicating the baseline sensor performance under unprocessed conditions. In contrast, Figure 6b shows the results after

applying the Savitzky–Golay smoothing filter, which significantly enhances the SNR to 172.18. The application of this smoothing algorithm notably improves the signal clarity by reducing high-frequency noise, resulting in a cleaner and more accurate signal representation. Furthermore, the maximum SNR achieved with the Savitzky–Golay smoothing is approximately 1.84 times higher than the SNR obtained without the smoothing filter. This substantial improvement in SNR directly translates to enhanced sensor sensitivity, allowing for the detection of even lower concentrations. As a result, the detection accuracy of CH_4 is reduced to 0.53 ppm, demonstrating the effectiveness of the S-G smoothing filter in significantly improving the sensor performance.

To further verify the effectiveness of the S-G filter smoothing denoising algorithm, it is compared with two traditional noise reduction methods, Kalman filter noise reduction and moving average noise reduction. The direct absorption signal obtained after denoising is compared with the fitted signal curve, and the noise reduction results for each algorithm are shown in Figure 6c,d. The parameters derived from the comparison of the denoising performance of the various algorithms are summarized in Table 1. The results demonstrate that, compared to the other two methods, the root mean square error (RMSE) of the direct absorption curves obtained using the S-G filter smoothing algorithm is significantly reduced by 0.000453, the signal-to-noise ratio (SNR) is notably increased by 172.18, and the correlation is greatly enhanced, with a correlation coefficient (CC) of 99.9533%. Consequently, the direct absorption signal curve processed with the S-G filter smoothing denoising method is much closer to the fitted curve. This method shows clear noise reduction advantages, effectively restoring the peak position of the direct absorption signal while preserving its authenticity.
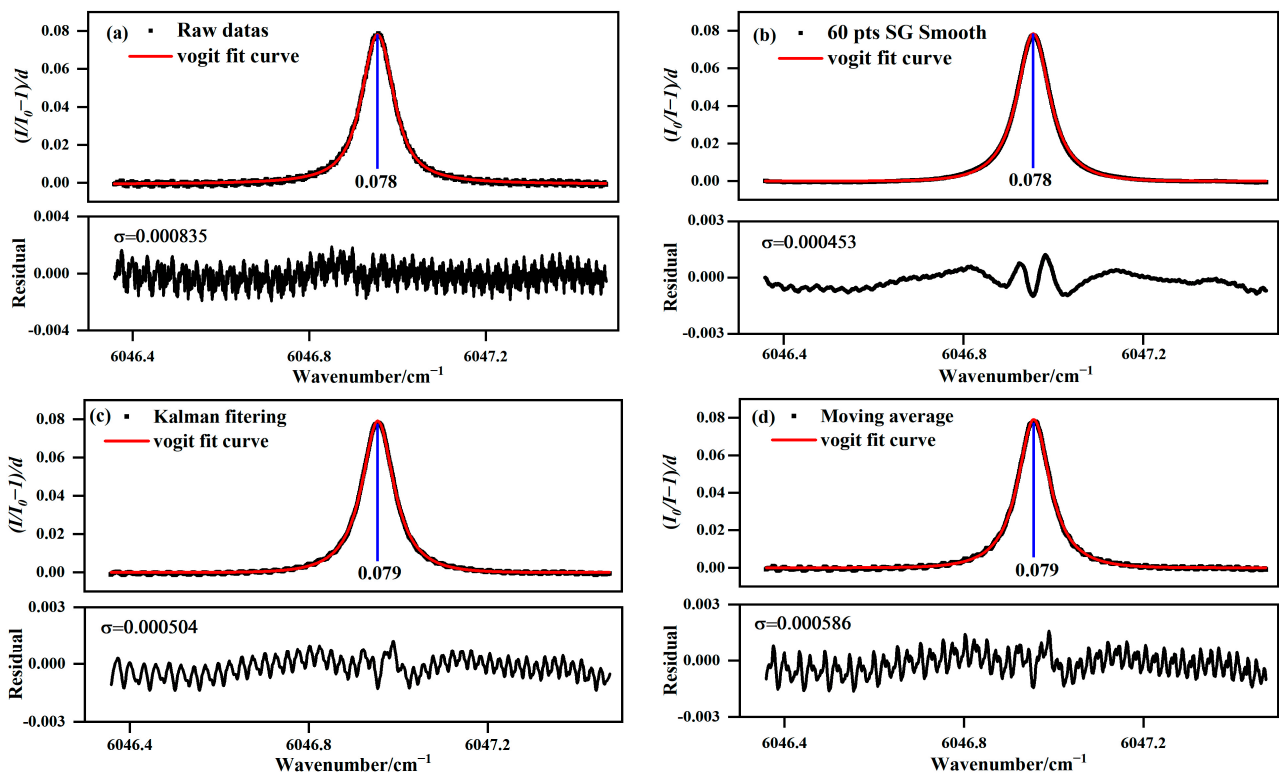
Figure 6. (**a**) The original signal. (**b**) The S-G smoothing signal. (**c**) Kalman filtering signal. (**d**) Moving average signal.

Table 1. Comparison of denoising effect.

Denoising Method	RMSE	SNR	CC/%
Raw data	8.35×10^{-4}	93.41	99.7736
60 pts SG Smooth	4.53×10^{-4}	172.18	99.9533
Kalaman filtering	5.04×10^{-4}	156.74	99.9014
Moving average	5.86×10^{-4}	134.81	99.8537

4. Conclusions

This paper presents an optical detection scheme for methane based on tunable diode laser absorption spectroscopy. Due to the degradation of signal quality from external noise, the Savitzky–Golay convolution smoothing algorithm was applied to the spectral data as a secondary processing step. This significantly enhanced the signal-to-noise ratio (SNR), improving the accuracy and reliability of the measurements. After applying the S-G smoothing, the SNR increased from an initial value of 93.41 to 172.18, which resulted in a CH_4 detection accuracy of 0.53 ppm. These results demonstrate the effectiveness of the system in detecting low-concentration methane, underscoring its potential for trace methane analysis in both environmental monitoring and industrial applications.

Author Contributions: Conceptualization, X.T., S.C. and G.C.; methodology, X.T.; software, S.C.; validation, J.Y., X.C. and S.C.; formal analysis, T.M. and S.C.; writing—original draft preparation, S.C.; writing—review and editing, X.T.; supervision, X.T., S.C. and G.C.; project administration, X.T. and G.C.; funding acquisition, X.T. and G.C. All authors have read and agreed to the published version of the manuscript.

Institutional Review Board Statement: Not applicable.

Informed Consent Statement: Not applicable.

Data Availability Statement: Data are contained within the article.

Conflicts of Interest: The authors declare no conflicts of interest.

References

1. Wilson, C. Untangling variations in the global methane budget. *Commun. Earth Environ.* **2023**, *4*, 318. [CrossRef]
2. Panagiotis, S.; Giannis, P.; Michalis, V. Remote Operation of an Open-Path, Laser-Based Instrument for Atmospheric CO_2 and CH_4 Monitoring. *Photonics* **2023**, *10*, 386. [CrossRef]
3. Srivastava, R.; Kedia, S.; Rajesh, T.A. Contribution of natural and anthropogenic aerosols to optical properties and radiative effects over an urban location. *Environ. Res. Lett.* **2012**, *7*, 034028.
4. Maazallahi, H.; Delre, A.; Scheutz, C.; Fredenslund, A.M.; Schwietzke, S.; van der Gon, H.D.; Röckmann, T. Intercomparison of detection and quantification methods for methane emissions from the natural gas distribution network in Hamburg, Germany. *Atmos. Meas. Tech.* **2023**, *16*, 5051–5073. [CrossRef]
5. Chen, J.Y.; Cui, P.X.; Zhou, C.C.; Yu, X.Y.; Wu, H.H.; Jia, L.Q.; Zhou, M.; Zhang, H.J.; Teng, G.E.; Cheng, S.; et al. Detection of CO_2 and CH_4 Concentrations on a Beijing Urban Road Using Vehicle-Mounted Tunable Diode Laser Absorption Spectroscopy. *Photonics* **2023**, *10*, 938. [CrossRef]
6. Wang, R.F.; Huang, T.X.; Mei, J.X.; Wang, G.S.; Liu, K.; Chen, W.D.; Gao, X.M. Pressure sensing with two-color laser absorption spectroscopy for combustion diagnostics. *Opt. Lett.* **2024**, *49*, 1033–1036. [CrossRef] [PubMed]
7. Shi, Y.P.; Hu, Z.; Niu, M.S.; Li, T.H.; Li, H.; Liu, H.Y.; Li, X.X. High-sensitive double incidence multi-pass cell for trace gas detection based on TDLAS. *Sens. Actuators B Chem.* **2024**, *412*, 135829. [CrossRef]
8. Masiyano, D.; Hodgkinson, J.; Schilt, S.; Tatam, R.P. Self-mixing interference effects in tunable diode laser absorption spectroscopy. *Appl. Phys. B* **2009**, *96*, 863–874. [CrossRef]

9.   Hartmann, A.; Strzoda, R.; Schrobenhauser, R.; Weigel, R. Ultra-compact TDLAS humidity measurement cell with advanced signal processing. *Appl. Phys. B* **2013**, *115*, 263–268. [CrossRef]

10.   Li, C.L.; Guo, X.Q.; Ji, W.H.; Wei, J.L.; Qiu, X.B.; Ma, W.G. Etalon fringe removal of tunable diode laser multi-pass spectroscopy by wavelet transforms. *Opt. Quant. Electron.* **2018**, *50*, 275.1–275.11. [CrossRef]

11.   Guo, X.Q.; Qiu, X.B.; Ji, W.H.; Shao, L.G.; Liu, S.P.; Li, C.L.; Ma, W.G. Minimization of Interference Fringes in Tunable Diode Laser A bs orption Spectrum Based on Empirical Mode Decomposition. *Laser Optoelectron. Prog.* **2018**, *55*, 113001.

12.   Dombi, J.; Dineva, A. Adaptive Savitzky-Golay filtering and its applications. *Int. J. Adv. Intell.* **2020**, *16*, 145–156. [CrossRef]

13.   Fábián, G. Generalized Savitzky–Golay filter for smoothing triangular meshes. *Comput. Aided Geom. Des.* **2023**, *100*, 102167. [CrossRef]

14.   Li, J.S.; Deng, H.; Li, P.F.; Yu, B.L. Real-time infrared gas detection based on an adaptive Savitzky–Golay algorithm. *Appl. Phys. B* **2015**, *120*, 207–216. [CrossRef]

15.   Tong, C.; Sima, C.; Chen, M.Q.; Zhang, X.H.; Li, T.L.; Ai, Y.; Lu, P. Laser Linewidth Analysis and Filtering/Fitting Algorithms for Improved TDLAS-Based Optical Gas Sensor. *Sensors* **2023**, *23*, 5130. [CrossRef] [PubMed]

16.   Yuan, Z.H.; Huang, Y.B.; Zhong, P.; Lu, X.J.; Huang, J.; Zhang, L.L.; Qi, G.; Cao, Z.S. Design and Study of Absorption Spectrum Measurement Device with V-Shaped Off-Axis Integrated Cavity. *Chin. J. Lasers* **2023**, *50*, 207.

17.   Ji, J.L.; Huang, Y.J.; Pi, M.Q.; Zhao, H.; Peng, Z.H.; Li, C.G.; Wang, Q.; Zhang, Y.; Wang, Y.D.; Zheng, C.T. Performance improvement of on-chip mid-infrared waveguide methane sensor using wavelet denoising and Savitzky-Golay filtering. *Infrared Phys. Technol.* **2022**, *127*, 04469. [CrossRef]

18.   Tian, X.; Cao, Y.; Chen, J.J.; Liu, K.; Wang, G.S.; Gao, X.M. Hydrogen sulphide detection using near-infrared diode laser and compact dense-pattern multipass cell. *Chin. Phys. B* **2019**, *28*, 063301. [CrossRef]

19.   Kochanov, R.V.; Gordon, I.E.; Rothman, L.S.; Shine, K.P.; Sharpe, S.W.; Johnson, T.J.; Wallington, T.J.; Harrison, J.J.; Bernath, P.F.; Birk, M.; et al. Infrared absorption cross-sections in HITRAN2016 and beyond: Expansion for climate, environment, and atmospheric applications. *J. Quant. Spectrosc. Radiat. Transfer.* **2019**, *238*, 106708. [CrossRef]

20.   Liu, K.; Wang, L.; Tan, T.; Wang, G.S.; Zhang, W.J.; Chen, W.D.; Gao, X.M. Highly sensitive detection of methane by near-infrared laser absorption spectroscopy using a compact dense-pattern multipass cell. *Sens. Actuators B Chem.* **2015**, *220*, 1000–1005. [CrossRef]